Improved Hairpin Resonator for Microfluidic Sensing

Chia-Feng Liu,[1] Ming-Kun Chen,[1] Min-Haw Wang,[2] and Ling-Sheng Jang[1*]

[1]Department of Electrical Engineering, National Cheng Kung University,
East Dist., Tainan, 70101, Taiwan
[2]Department of Electrical Engineering, Chinese Culture University,
Shilin Dist., Taipei, 11114, Taiwan

We present a near-field microwave sensor based on a hairpin resonator for detecting aqueous ethanol and aqueous NaCl concentrations in microfluidics. A hairpin sensor with a high-quality (high-Q) dielectric resonator allows the detection of a small variation in the aqueous NaCl concentration by measuring the scattering parameter (S_{21}) responses at resonance frequencies. The responses caused by the test liquids with various dielectric constants in aqueous ethanol solution were observed at operating frequencies of 1.9 and 2.1 GHz. The detection of various concentrations of NaCl in solution was also achieved. The changes in S_{21} at resonance frequencies are directly related to changes in the aqueous NaCl concentration because of the electromagnetic interaction between the resonator and the NaCl solution. The stable linear relationships are advantageous for detecting and analyzing aqueous ethanol and aqueous NaCl concentrations. It shows that the sensor is reliable for both dielectric constant and conductivity detection in liquid. The hairpin resonator, which is easily fabricated by standard printed circuit board (PCB) technology, has great potential for microfluidic sensing applications.

1. Introduction

Impedance measurement is one of the most promising techniques for developing label-free, real-time, and noninvasive methods of detection. Many sensors have been built for the detection of biotissues, and fluid concentrations such as those in biological cells, glycated hemoglobin (HbA$_{1c}$), glucose solution, and NaCl solution.[1–8] However, at low frequencies, the contact area of the electrode-solution, tissue-solution, and tissue-electrode interfaces produces the electric double-layer capacitance effect, which influences the measured impedance.[9,10] It is difficult to obtain the precise properties of biomaterials at low frequencies. In the low frequency range, the electrical response of the system is dominated by electrical double layer capacitance. In order to analyze and verify the measurement results obtained at low frequencies, the surface-specific double-layer capacitance effect must be included in the equivalent circuit model. It is difficult to obtain the precise properties of biotissues or medical indices. Moreover, at frequencies above 100 MHz, the interaction of microwaves and biological tissues is almost exclusively dependent

on the aqueous and ionic content. It is very useful to have accurate values of the properties of biological tissues at these frequencies.[11]

Microwave sensing technology has been successfully used for measurement and detection. Many research groups designed sensors that operate at microwave frequencies to reduce the electric double-layer capacitance effect and enhance the accuracy of detection. A coplanar waveguide probe was built to perform single-HeLa-cell impedance measurements over the frequency range of 1.0 MHz to 1.0 GHz.[12] Impedance sensors with nanometer gaps were prepared for the detection of biomolecular interactions such as protein-antibody and protein-aptamer binding.[13]

In addition, microwave resonant structures are used for developing noninvasive detection techniques. The microwave resonator, which is widely used for communication systems, is the most suitable microwave component for building a biosensor.[14,15] A high-Q resonator can be applied to achieve high-sensitivity detection at a specific frequency. Many sensors composed of microwave resonators were designed to detect the electromagnetic wave interaction with water-based substances or biological materials. A planar microwave filter was utilized for biological cell discrimination by impedance spectroscopy analysis at microwave frequencies.[16] A method of biomolecule detection where a double split-ring resonator excited by a microstrip transmission line is used was proposed.[17] An electromagnetic resonant spiral sensor was designed for noninvasive D-glucose detection.[18] An electromagnetic wave sensor operating in the 0.01 to 4.0 GHz range for real-time chloride concentration analysis was reported.[19] Thus, microwave technology has great potential for biosensing applications.

In the field of microwave communication technology, many types of resonator, such as end-coupled resonators, parallel-coupled resonators, interdigital coupled-line resonators, and dielectric resonators, are used for building microwave filters.[20–22] However, the circuit size of conventional planar microwave resonators is large. A greater volume of the liquid under test (LUT) for measurement is required. In this study, hairpin resonators are first used for microfluidic sensing. We use a near-field microwave filter to construct a miniaturized hairpin sensor, which is half the size of a conventional hairpin resonator, for detecting aqueous NaCl concentration.[23] The detection with only a 7.7 μL volume of LUT was achieved. NaCl concentration is an important index in pathology, biology, food processing, and seawater detection.[24,25] NaCl in aqueous solution is often used as a standard liquid in experiments to measure the dielectric properties of biological material, because biological tissues typically have a high water content and a significant concentration of ions.[11] In addition, different from the above studies that worked on single kind of liquid, this work performs detection of both aqueous ethanol and aqueous NaCl concentrations. The linear S_{21} responses with dielectric constant and conductivity of liquid can be both achieved by the same hairpin sensor. Moreover, the microfluidic sensor with single-layer electrodes has many advantages: easily fabricated by standard PCB technology, low-cost, high reliability, fast response, and real-time detection. Thus, the hairpin resonator has great potential for microfluidic sensing applications.

2. Design and Fabrication

2.1 Design basis

The spectra at GHz frequencies of deionized (DI) water and NaCl, KCl, $MnCl_2$, and CuCl solutions of various concentrations were recorded with a microwave sensor.[19,26,27] Radiation at microwave frequencies between 1.5 and 5.0 GHz is only slightly attenuated by atmospheric gases.[28] It has been observed that the frequency range of 0.5 to 4.0 GHz is best suited for salinity estimation.[29] The presence and concentration of various chloride solutions are also clearly evident in the changes in the amplitude and resonance frequency of the signal occurring especially at frequencies below 4.0 GHz. Moreover, for aqueous alcohols, the relative permittivity is dependent on the frequency. Above 2.2 GHz, as the frequency increases, the real part of complex permittivity decreases towards its high-frequency-limit relative permittivity value, and the imaginary part of complex permittivity increases to a peak value.[30] According to the above, a microwave hairpin resonator sensor that operates at 1.9 and 2.1 GHz for NaCl and ethanol detection, respectively, was designed in this work. The sensor is constructed of four hairpin-shaped half-wavelength stepped impedance resonators (SIRs) that create resonances as the sensing tool for the liquid detection, as shown in Fig. 1.[27] Design parameters of the sensor are shown in Table 1. The SIR sensor is a transverse electromagnetic (TEM-) or quasi-TEM-mode resonator composed of two or more transmission lines with different characteristic impedances. Good resonance conditions at a specific frequency can be achieved by adjusting the impedance ratio. The specific resonance frequency is determined by the lengths and the characteristic impedances of the resonator. In order to further reduce the size of the resonator, the SIR structure was transformed into a hairpin shape.[31]

Table 1
Design parameters of the hairpin resonator sensor.

Symbol	Description	Value	Units
ε_r	Substrate dielectric constant	3.38	—
tanδ	Substrate loss tangent	0.003	—
—	Substrate thickness	508	μm
W_1	Strip width	3220	μm
W_2	Strip width	2410	μm
W_3	Microstrip width	580	μm
W_4	Microstrip width	720	μm
W_5	Feed width	1140	μm
g_1	Gap of resonators	520	μm
g_2	Gap of coupled line	460	μm
g_3	Gap of resonators	610	μm
g_4	Gap of resonators	1750	μm
L_1	Strip length	8800	μm
L_2	Microstrip length	10560	μm
L_3	Microstrip length	5600	μm
L_4	Coupled line length	5530	μm
L_5	Microstrip length	7890	μm
L_6	Feed length	1730	μm
—	Copper thickness	35	μm

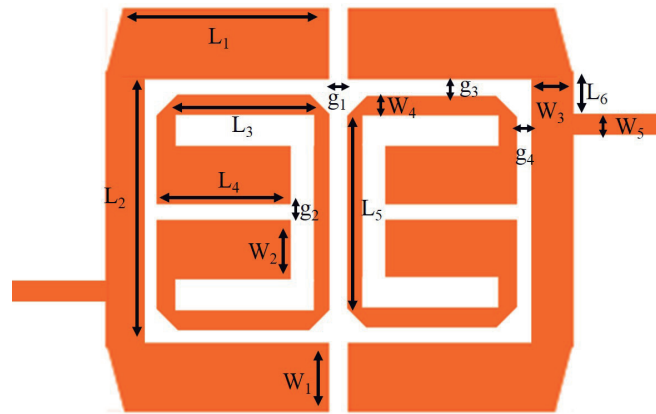Fig. 1.   (Color online) Geometry of the hairpin-shape resonator.

(a)   (b)
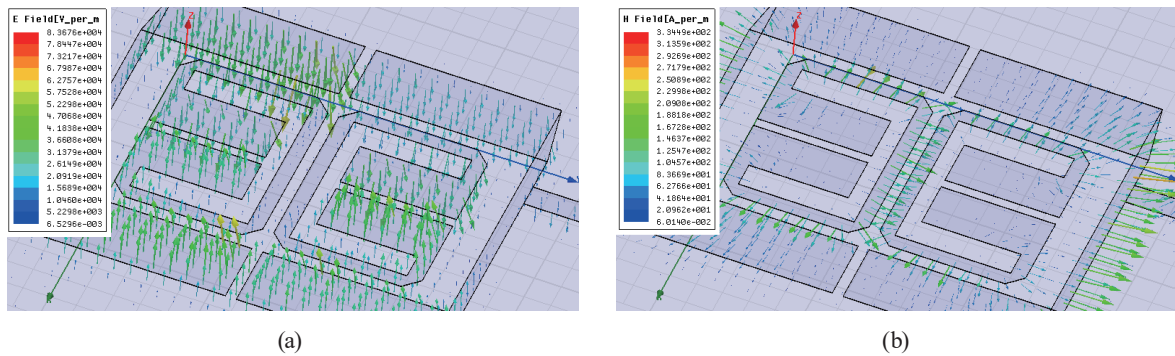
Fig. 2.   (Color online) (a) HFSS model of the electric field distribution. (b) HFSS model of the magnetic field distribution.

Figure 2 shows the simulation results of the electric and magnetic field distribution. The crosstalk between resonators was observed. The scattering parameters are related to the mutual capacitor that represents the interaction between resonators.[23] High sensitivity can be achieved by using the mutual capacitor as a sensing area. The mutual capacitor phenomenon was used to detect aqueous ethanol and aqueous NaCl concentrations.

2.2   Fabrication

The sensor was fabricated on a double-sided copper-clad Rogers RO4003C substrate with a thickness of 508 μm, a relative dielectric constant of 3.38, and a loss tangent of 0.0027. The electrodes were fabricated using a PCB engraving machine. The bottom copper layer acted as the ground plane. Then, a subminiature version A (SMA) adapter was soldered onto the board, with the center pin directly connected to the signal line and ground pins connected to the back ground planes. Tygon R-3603 laboratory tubing (inner diameter: 0.7 mm; outer diameter: 2.4 mm) for containing the medium was bonded onto the sensor. Figure 3 shows the photograph
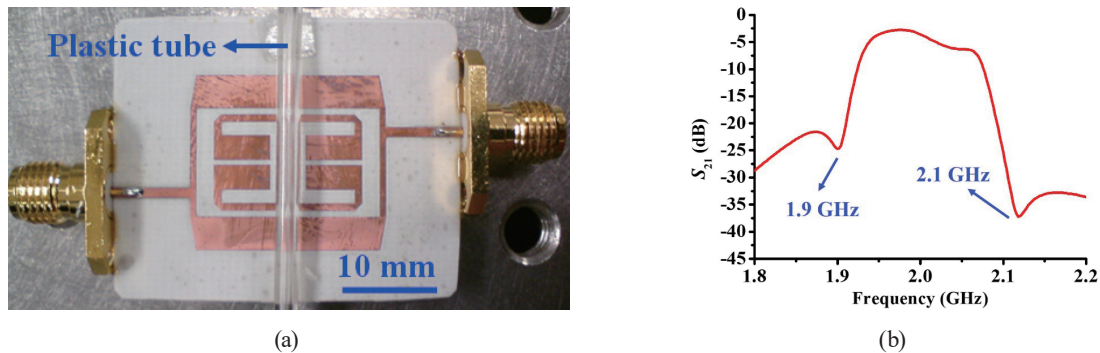
Fig. 3.   (Color online) (a) Photograph of hairpin resonator sensor and (b) measured resonances of the sensor.

and measured S_{21} responses of the sensor. The sensor has a center resonance at 2.0 GHz. The other two resonances occur at 1.9 and 2.1 GHz. These resonance conditions are suitable for the detection of liquid responses.

3.   Experimental Setup

At microwave frequencies, systematic effects such as leakage, test port mismatch, and frequency response can affect measurement data. In a stable measurement environment, these effects are reproducible and can be eliminated using the vector network analyzer (VNA) with a calibration procedure. In accordance with the fixture and the VNA used in this work, short-open-load-through (SOLT) calibration was used for this case. As shown in Fig. 4(a), a series of calibration structures, such as open, short, load, and through structures, were manufactured to improve the calibration accuracy. The 50 Ω matched load was realized by two 100 Ω SMD resistors connected in parallel to the ground plane, shown in Fig. 4(b). The calibration procedure was carried out by connecting a through kit, a load kit, a short kit, and an open kit to the desired test ports sequentially. All measurement instruments were controlled using a personal computer via a general-purpose interface bus line. The computer and custom-made software were used for automatic data acquisition and complex calculations.

The experiments were conducted at a temperature of 24 ± 1 °C under a relative humidity of 43 ± 10%. The fluid was injected into the tubing using a syringe and allowed to travel to the outlet of the tubing. Then, the response of the fluid was measured by the VNA (Agilent Technologies E5062A) shown in Fig. 4(c).

4.   Results and Discussions

4.1   Aqueous ethanol concentration detection

The measured S_{21} responses of ethanol and DI water are shown in Fig. 5(a). Changes in S_{21} caused by the medium can be observed at 1.9 and 2.1 GHz. Figures 5(b) and 5(c) show the detailed responses at 1.9 and 2.1 GHz, respectively. The measured S_{21} at 1.9 GHz increased
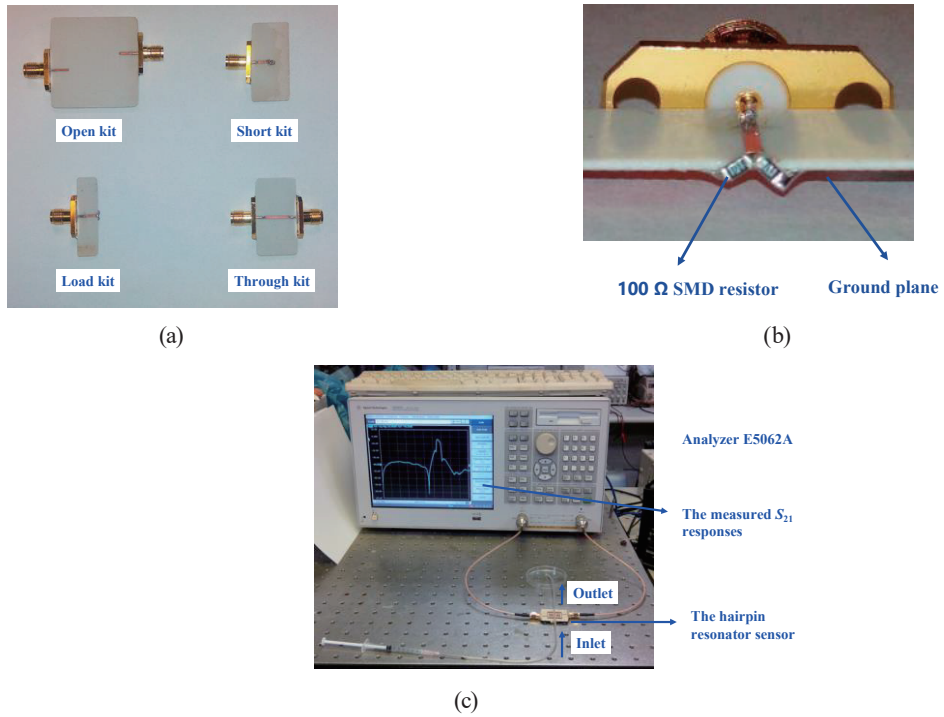
(a)

(b)

(c)

Fig. 4.   (Color online) (a) The used calibration kits. (b) The load kit. (c) View of the measurement setup.
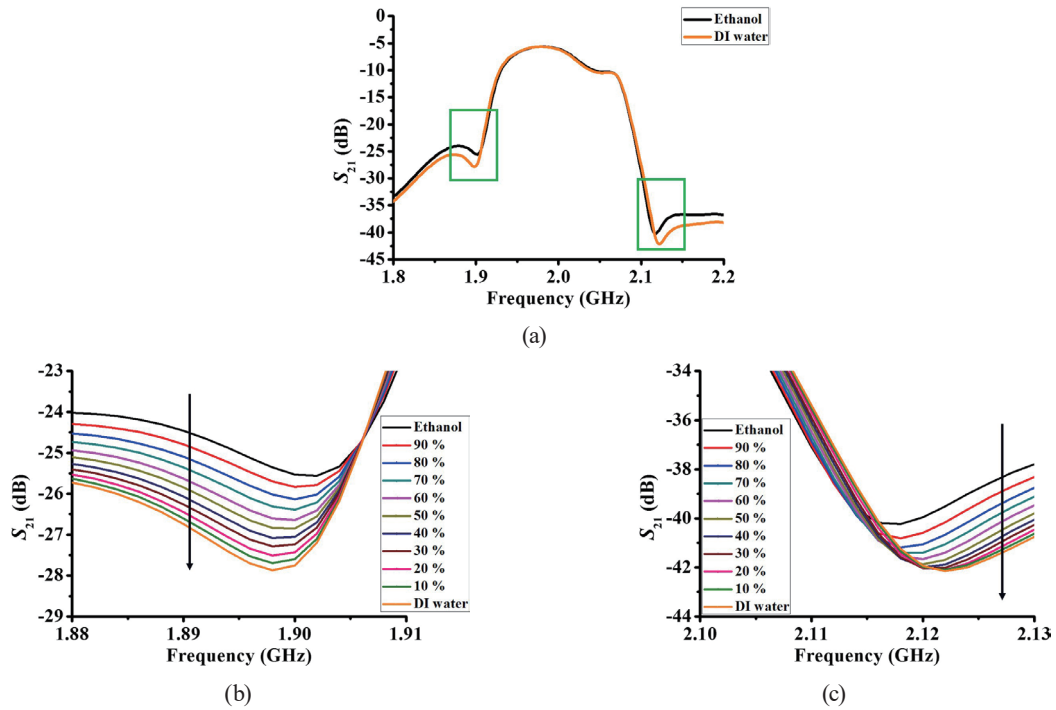

(a)

(b)

(c)

Fig. 5.   (Color online) (a) Measured S_{21} responses of ethanol and DI water. Detailed responses at (b) 1.9 and (c) 2.1 GHz.

with increasing concentration of aqueous ethanol solution from −27.9 dB for 0% to −25.6 dB for 100%. The measured S_{21} at 2.1 GHz also increased with increasing concentration of ethanol solution from −42.1 dB for 0% to −40.2 dB for 100%. The dielectric constant of aqueous ethanol solution decreases with increasing ethanol concentration.[32] According to coupled line theory, the coupling coefficient increases because of the larger capacitance between two coupled resonators. A high-dielectric-constant liquid directly causes the coupling capacitance to increase. At both resonances of 1.9 and 2.1 GHz, the larger dielectric constant of the LUT causes the greater attenuation. The variation of the dielectric constant of an LUT can be detected from the attenuation variation. Figure 6(a) shows the S_{21} responses of aqueous ethanol concentrations from DI water to ethanol at intervals of 10%. Regular changes in S_{21} occurred at 1.9 and 2.1 GHz. The changes in S_{21} at 1.9 GHz with the variation of the percentage of aqueous ethanol solution are more linear than those at 2.1 GHz. At 1.9 GHz, the S_{21} responses show a linearly increasing trend with increasing aqueous ethanol concentrations. The slope of the linear relationship between the S_{21} responses and the aqueous ethanol concentration was found to be 0.023 dB/%.

The dielectric constants of ethanol, 80% aqueous ethanol solution, 50% aqueous ethanol solution, and water are known to be about 23.6, 35.4, 51.2, and 79, respectively.[32] The measured S_{21} and the trend line at 1.9 GHz versus dielectric constant are plotted in Fig. 6(b). The coefficient of determination (R^2) was found to be 0.9954. The trend function is described by Eq. (1) where $S_{21,measured}$ is the measured S_{21} at 1.9 GHz. Then the dielectric constant of aqueous ethanol solution ($\varepsilon_{r,ethanol}$) can be derived as Eq. (2).
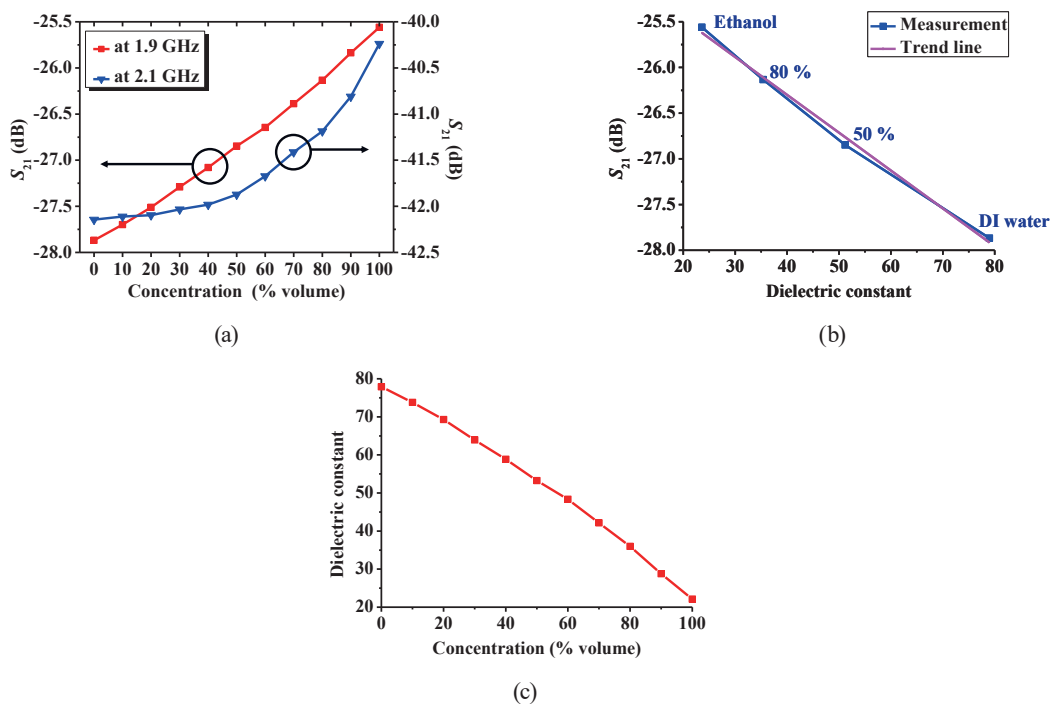

Fig. 6. (Color online) (a) Measured S_{21} responses of aqueous ethanol concentrations from DI water to ethanol at 1.9 and 2.1 GHz. (b) Measured S_{21} responses at 1.9 GHz and the trend line plotted as a function of dielectric constant. (c) Estimated dielectric constant as a function of the aqueous ethanol concentrations.

$$S_{21,measured} = -0.0414 \cdot \varepsilon_{r,ethanol} - 24.644 \qquad (1)$$

$$\varepsilon_{r,ethanol} = -\frac{S_{21,measured} + 24.644}{0.0414} \qquad (2)$$

The estimated dielectric constant as a function of the aqueous ethanol concentration is plotted in Fig. 6(c). It shows that the sensor can be used to detect the ethanol content in aqueous solution through dielectric constant detection.

4.2 Aqueous NaCl concentration detection

The conductivities of aqueous NaCl concentrations from DI water to 100 mg/mL were measured using a conductivity meter (Suntex SC-110). As shown in Fig. 7(a), a linear relationship between the concentration and conductivity was observed. The conductivity of aqueous sodium chloride solution increases with increasing sodium chloride concentration. The conductivity of the LUT influences the S_{21} responses because of the electromagnetic interaction between the sensor and the sodium chloride solution. Figure 7(b) shows the measured S_{21} responses of aqueous NaCl solution of various concentrations. Figures 7(c) and 7(d) show the detailed responses at 1.9 and 2.1 GHz, respectively. Regular changes in S_{21} occurred at 1.9 and 2.1
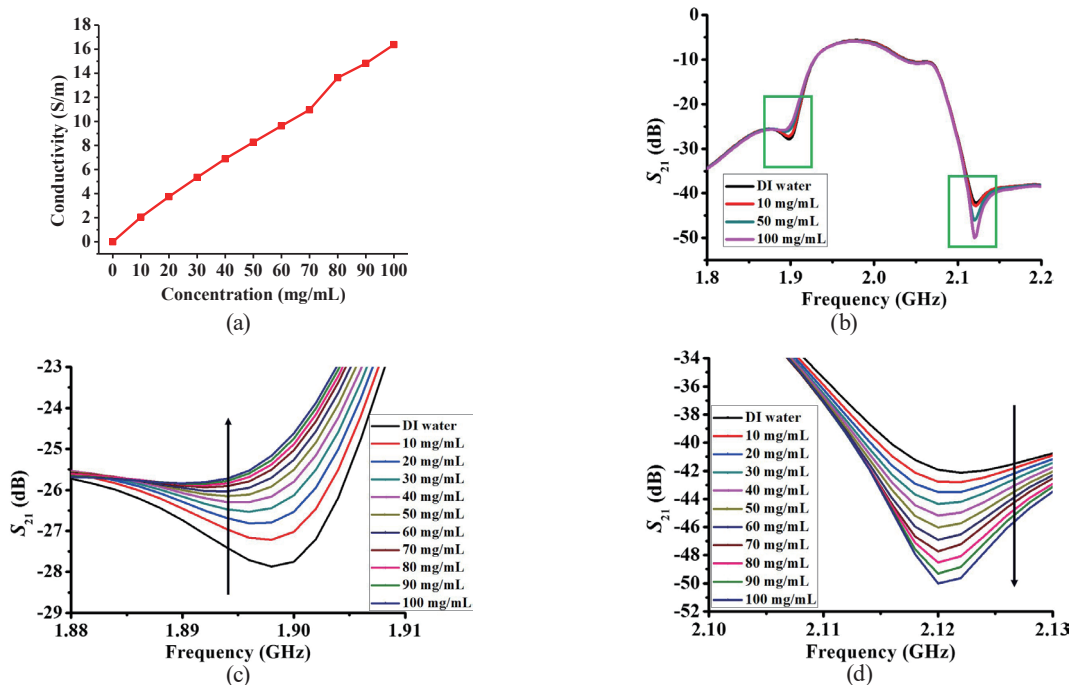

Fig. 7. (Color online) (a) Conductivity of aqueous NaCl solution with concentrations of 0 to 100 mg/mL. (b) Measured S_{21} responses of aqueous NaCl solution with various concentrations and DI water. Detailed responses at (c) 1.9 and (d) 2.1 GHz.

GHz. The measured S_{21} at 1.9 GHz increased with increasing concentration of NaCl solution from −27.9 dB for 0 mg/mL to −25.8 dB for 100 mg/mL. In contrast, the measured S_{21} at 2.1 GHz decreased with increasing concentration of NaCl solution from −42.1 dB for 0 mg/mL to −50.0 dB for 100 mg/mL. The greatest change in S_{21} was about 8 dB, which occurred at 2.1 GHz when the concentration was increased from 0 to 100 mg/mL. The detection resolution in mg/mL (R_{detect}) of the sensor is

$$R_{detect} = \left| \frac{\Delta c}{\Delta S_{21}} \right| \times R_{system}, \tag{3}$$

where Δc is the concentration variation in mg/mL, ΔS_{21} is the change in measured S_{21} in dB, and $R_{system} = 0.05$ dB is the resolution of the system. The detection resolution was found to be 0.63 mg/mL.

Moreover, the changes in S_{21} at 2.1 GHz are more linear than those at 1.9 GHz for various concentrations shown in Figs. 8(a) and 8(b). At 2.1 GHz, the linear relationship between S_{21} responses and aqueous NaCl concentration, $|\Delta S_{21}/\Delta c|$, was found to be 0.082 dB/(mg/mL) in the range of 10 to 100 mg/mL and 0.069 dB/(mg/mL) in the range of 0 to 10 mg/mL.

In addition, the measured S_{21} and the trend line at 2.1 GHz versus conductivity are plotted in Figs. 8(c) and 8(d). The linear relationship between S_{21} and conductivity suitable for low concentrations (1 to 10 mg/mL) is described by Eq. (4). The sensitivity and R^2 were found to
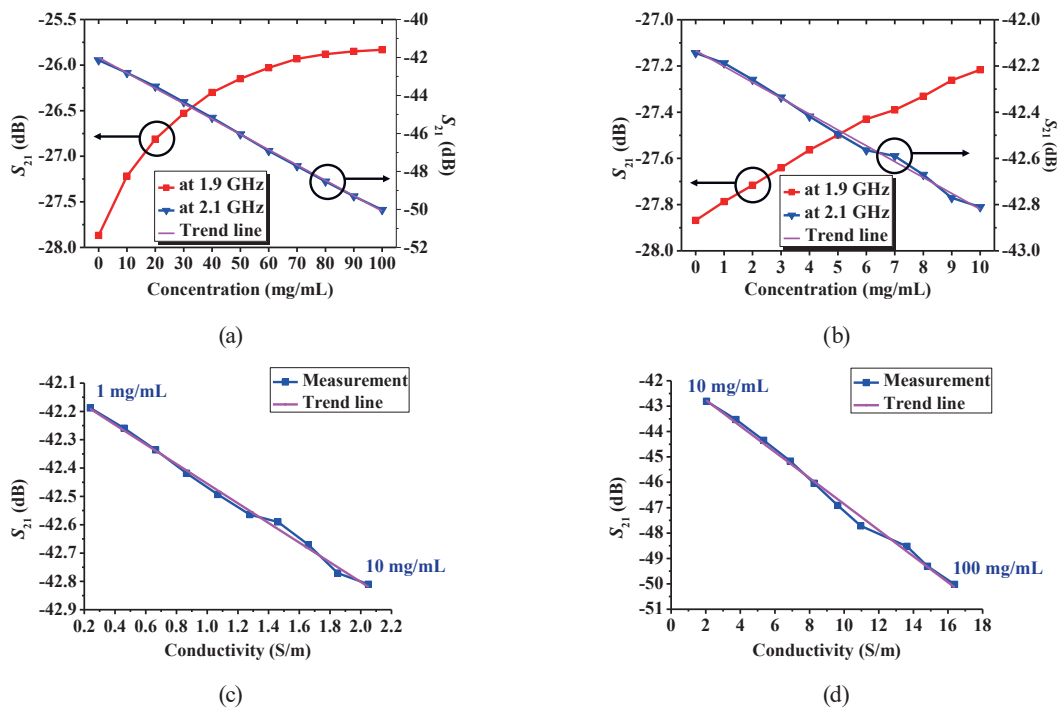

Fig. 8. (Color online) (a) Measured S_{21} responses of aqueous NaCl concentrations ranging from 0 to 100 mg/mL and (b) from 0 to 10 mg/mL at 1.9 and 2.1 GHz. (c) Measured S_{21} responses at 2.1 GHz and the trend line plotted as a function of conductivity for the aqueous NaCl concentrations from 1 to 10 mg/mL and (d) 10 to 100 mg/mL.

be 0.3385 dB/(S/m) and 0.9948, respectively. Moreover, the linear relationship between S_{21} and conductivity suitable for high concentrations (10 to 100 mg/mL) is described by Eq. (5). The sensitivity and R^2 were found to be 0.5132 and 0.9956 dB/(S/m), respectively, which are higher than those at low concentrations.

$$S_{21,measured} = -0.3385 \cdot \sigma_{NaCl} - 42.12 \tag{4}$$

$$S_{21,measured} = -0.5132 \cdot \sigma_{NaCl} - 41.729 \tag{5}$$

These stable linear relationships are helpful for detecting and analyzing aqueous NaCl concentrations. The sensor is thus suitable for biodetection applications.

5. Conclusions

We used miniaturized hairpin resonators with two resonances to determine aqueous ethanol and aqueous NaCl concentrations. The LUT was analyzed by observing the variation in scattering parameters at resonance frequencies. The S_{21} was sensitive to the concentrations of aqueous ethanol and aqueous NaCl and had a linear relationship in the entire concentration range. The slope of the linear relationship between S_{21} responses and aqueous ethanol concentrations at 1.9 GHz was found to be 0.023 dB/%. A prototype sensor was used to demonstrate the measurement method for various concentrations of aqueous NaCl. The detection resolution was 0.63 mg/mL with a 7.7 μL volume at operating frequencies of 1.9 and 2.1 GHz. The slopes of the linear relationships between S_{21} responses and aqueous NaCl concentrations at 2.1 GHz were found to be 0.069 dB/(mg/mL) in the range of 0 to 10 mg/mL and 0.082 dB/(mg/mL) in the range of 10 to 100 mg/mL. In summary, the sensor is linearly sensitive to the dielectric constant of solution at 1.9 GHz and to the conductivity of solution at 2.1 GHz. These results show that the microwave hairpin resonator sensor can be applied to both dielectric liquid and aqueous NaCl detection. These stable linear relationships are advantageous for biodetection applications. Another advantage is the possibility of a planar structure, which is well suited for biosensor applications. Standard PCB fabrication technologies can be used to produce low-cost biosensing devices.

References

1 A. Yúfera, A. Rueda, J. M. Muñoz, R. Doldán, G. Leger, and E. O. Rodríguez-Villegas: IEEE Trans. Circuits Syst. Regul. Pap. **52** (2005) 2620.
2 S. G. Badhe and S. N. Helambe: Sci. Res. Rep. **3** (2013) 239.
3 L. S. Jang and M. H. Wang: Biomed. Microdevices **9** (2007) 737.
4 Y. Cho, H. S. Kim, A. B. Frazier, Z. G. Chen, D. M. Shin, and A. Han: J. Microelectromech. Syst. **18** (2009) 808.
5 J. L. Hong, K. C. Lan, and L. S. Jang: Sens. Actuators, B **173** (2012) 927.
6 Y. C. Chuang, K. C. Lan, K. M. Hsieh, L. S. Jang, and M. K. Chen: Sens. Actuators, B **171–172** (2012) 1222.
7 G. Yoon: Biosens. Bioelectron. **26** (2011) 2347.
8 P. Mirtaheri, S. Grimnes, and Ø. G. Martinsen: IEEE Trans. Biomed. Eng. **52** (2005) 2093.
9 D. E. Yates, S. Levine, and T. W. Healy: J. Chem. Soc., Faraday Trans. 1 **70** (1974) 1807.
10 T. Sun, N. G. Green, and H. Morgan: Nano **3** (2007) 55.
11 A. Peyman, C. Gabriel, and E. H. Grant: Bioelectromagnetics **28** (2007) 264.
12 J. Y. Jao, C. F. Liu, M. K. Chen, Y. C. Chuang, and L. S. Jang: Microelectron. Reliab. **51** (2011) 781.
13 M. Lohndorf, U. Schlecht, T. M. A. Gronewold, A. Malave, and M. Tewes: Appl. Phys. Lett. **87** (2005) 243902.
14 J. S. Hong, M. J. Lancaster, D. Jedamzik, and R. B. Greed: IEEE MTT-S Int. (IEEE, Baltimore, 1998) 367.
15 F. A. Miranda, G. Subramanyam, F. W. van Keuls, R. R. Romanofsky, J. D. Warner, and C. H. Mueller: IEEE Trans. Microwave Theory Tech. **48** (2000) 1181.
16 C. Dalmay, M. Cheray, A. Pothier, F. Lalloué, M. O. Jauberteau, and P. Blondy: Sens. Actuators, A **162** (2010) 189.
17 H. J. Lee, H. S. Lee, K. H. Yoo, and J. G. Yook: J. Appl. Phys. **108** (2010) 014908.
18 H. Melikyan, E. Danielyan, S. Kim, J. Kim, A. Babajanyan, J. Lee, B. Friedman, and K. Lee: Med. Eng. Phys. **34** (2012) 299.
19 O. Korostynska, M. Ortoneda-Pedrola, A. Mason, and A.I. Al-Shamma'a: Meas. Sci. Technol. **25** (2014) 065105.
20 R. W. Rhea: HF Filter Design and Computer Simulation (Noble Publishing, Atlanta, 1994).
21 J. S. Hong and M. J. Lancaster: Microstrip Filters for RF Microwave Applications (John Wiley & Sons, New York, 2001).
22 M. Sagawa, K. Takahashi, and M. Makimoto: IEEE Trans. Microwave Theory Tech. **37** (1989) 1991.
23 S. Y. Lee and C. M. Tsai: IEEE Trans. Microwave Theory Tech. **48** (2000) 2482.
24 I. M. S. Lampreia, S. R. J. Magalhaes, S. I. M. Rodrigues, and A. F. S. S. Mendonca: J. Chem. Thermodyn. **38** (2006) 240.
25 L. Mayor, R. Moreira, F. Chenlo, and A. M. Sereno: J. Food Eng. **74** (2006) 253.
26 M. Ortoneda-Pedrola, O. Korostynska, A. Mason, and A. I. Al-Shamma'a: J. Phys. Conf. Ser. **450** (2013) 012016.
27 M. Ortoneda-Pedrola, O. Korostynska, A. Mason, and A. I. Al-Shamma'a: J. Phys. Conf. Ser. **450** (2013) 012013.
28 H. J. C. Blume, A. W. Love, M. J. van Melle, and W. W. Ho: IEEE J. Oceanic Eng. **2** (1977) 121.
29 R. P. Singh, V. Kumar, and S. K. Srivastav: Int. J. Remote Sens. **11** (1990) 321.
30 R. L. Smith Jr., S. B. Lee, H. Komori, and K. Arai: Fluid Phase Equilib. **144** (1998) 315.
31 M. Makimoto and S. Yamashita: Microwave Resonators and Filters for Wireless Communication (Springer, Berlin, 2000).
32 M. I. Khalil and S. I. Al-Resayes: Int. J. Phys. Sci. **7** (2012) 578.

About the Authors

Chia-Feng Liu is currently a Ph.D. student in the Department of Electrical Engineering, National Chen Kung University, Taiwan. He received his B.S. and M.S. degrees from the Department of Electrical Engineering, National Chen Kung University, Taiwan, in 2007 and 2010, respectively. His research focuses on the design and fabrication of microfluidic devices integrated with microwave resonators for single-cell measurement and analysis at radio frequencies.

Ming-Kun Chen received his Bachelor's degree in electronic engineering from National Yunlin University of Science and Technology, Yunlin, Taiwan, in 1995, Master's degree in electronic engineering from I-Shou University, Kaohsiung, Taiwan, in 2002, and Ph.D. degree while at the Nondestructive Evaluation (NDE) Laboratory of the Electrical Engineering Department, National Cheng Kung University, Tainan, Taiwan, in 2006. From 1996 to 2002, he was at Advanced Semiconductor Engineering Test (ASET) Ltd., Kaohsiung, where he worked on IC testing interfaces and testing technology improvement. His research interests are in the areas of high-speed measurement, modeling, simulation methodology of packaging, the development of silicon sensor chips, microfluid handling systems for the measurement of living cells with microsensor systems, failure analysis of IC packaging/testing, analysis of signal integrity, and nondestructive testing.

Min-Haw Wang is currently an associate professor in the Department of Electrical Engineering at Chinese Culture University in Taiwan. He received his B.S. degree in electrical engineering at Chinese Culture University in 2000 and his M.S. degree in electrical engineering at National Tsing Hua University in 2003. He received his Ph.D. from the Department of Electrical Engineering, National Chen Kung University, Taiwan, in 2010. His current research focuses on microfluidics for biomedical applications.

Ling-Sheng Jang is currently a professor in the Department of Electrical Engineering at National Cheng Kung University in Taiwan. He received his B.S. degree in marine mechanical engineering at National Taiwan Ocean University in 1992 and his M.S. degree in mechanical engineering at National Chiao-Tung University in 1994. He received his Ph.D. in mechanical engineering from the University of Washington, Seattle, WA, in 2003. His current research focuses on microfluidics for biomedical applications.